J. Braz. Chem. Soc., Vol. 22, No. 4, 718-725, 2011.
Printed in Brazil - ©2011 Sociedade Brasileira de Química
0103 - 5053 $6.00+0.00

Article

Nanoporous of W/WO_3 Thin Film Electrode Grown by Electrochemical Anodization Applied in the Photoelectrocatalytic Oxidation of the Basic Red 51 used in Hair Dye

Luciano E. Fraga* and Maria Valnice B. Zanoni

Departamento de Química Analítica, Instituto de Química, Universidade Estadual Paulista, 14800-900 Araraquara-SP, Brazil

Eletrodo nanoporoso auto-organizado de W/WO_3 pode ser obtido através da anodização eletroquímica de placas de W em solução de NaF 0,15 mol L^{-1} como eletrólito suporte, aplicando uma rampa de potencial de 0,2 V s^{-1}, até alcançar 60 V, mantendo por 2 h. A forma monoclínica altamente ordenada do WO_3 é majoritária quando calcinado a 450 ^{0}C durante 30 min, obtendo uma maior fotoatividade quando irradiada na luz visível em relação a luz UV. O eletrodo promove a descoloração total do vermelho básico 51, utilizado em tinturas de cabelo, após 60 min de oxidação fotoeletrocatalítica, em densidade de corrente de 1,25 mA cm^{-2} e irradiação em comprimento de onda 420-630 nm. Nessa condição foi obtido 63% de mineralização. Uma menor eficiência é obtida para o sistema irradiado por comprimento de onda (280-400 nm), quando apenas 40% de remoção de carbono orgânico total é obtida, necessitando de 120 min de tratamento para a descoloração total da solução do vermelho básico 51.

Self-organized W/WO_3 nanoporous electrodes can be obtained by simple electrochemical anodization of W foil in 0.15 mol L^{-1} NaF solution as the supporting electrolyte, applying a ramp potential of 0.2 V s^{-1} until it reached 60 V, which was maintained for 2 h. The monoclinic form is majority in the highly ordered WO_3 annealed at 450 $^{\circ}$C, obtaining a higher photoactivity when irradiated by visible light than by UV light. The electrode promotes complete discoloration of the investigated basic red 51 dye after 60 min of photoelectrocatalytic oxidation, on current density of 1.25 mA cm^{-2} and irradiation on wavelength of 420-630 nm. In this condition it was obtained 63% of mineralization. Lower efficiency is obtained for the system irradiated by wavelength (280-400 nm) when only 40% of total organic carbon removal is obtained and 120 min is required for complete discoloration.

Keywords: W/WO_3 electrodes, electrochemical anodization, photoelectrocatalysis, basic red 51, hair dye

Introduction

The use of TiO_2 as photoanode in photoelectrocatalytic degradation of pollutants is well known in literature.[1-10] Nevertheless, this material presents band gap energy around 3.2 eV, which is photoexcited only in the ultraviolet region ($\lambda \leq 380$ nm).[11-14] Tungsten trioxide has been an excellent alternative material, since it presents smaller band gap energy (2.4-2.8 eV) and can be photoexcited in the visible region close to the UV region.[15-18] However, most of the studies found in literature explore tungsten trioxide only as electrochromic applications and solar energy conversion.[1] WO_3 films have been prepared using several techniques, *e.g.*: vacuum evaporation,[19] chemical vapor,[20,21] sol-gel precipitation,[22-25] spin coating,[26] sputtering,[27] and electrodeposition.[28-34] Although a sol-gel technique is one of the simplest and lowest-cost procedures selected for a wide range of applications, there have been only a few reports on photoelectrochemical characteristics of the WO_3 film prepared by a sol-gel technique.[5-8]

Several techniques for improving photoresponse of thin film electrodes W/WO_3 have already been proposed. The electrodeposited Pt/WO_3 catalysts have improved the oxidation of methanol and formic acid.[35-38] The WO_x films with Pt, Sn, and Ru dopands were used for electrooxidation of acetaldehyde. Some authors have described the photoelectrocatalytic degradation of Remazol Black B dye, methylene blue and 4-chlorophenol in aqueous solutions by using *n*-WO_3 photoelectrode activated by ultraviolet irradiation.[39-42] In general, the systems exhibited

*e-mail: fraga@iq.unesp.br

higher degradation rate as well as the increased extent of degradation. However, studies focused on photocatalytical and photoelectrocatalytical processes using activation in the visible region are scarce, limiting to purification of water[39] and oxidation of some organics.[28,40,41,43]

The basic red 51 dye, Figure 1, is a soluble dye widely used in several commercial formulations destined to semi-permanent hair dyeing.[44] They are used as temporarily molecules deposited in the external structure of the hair by ionic forces involving interaction with protein fibers of the hair.[45] The release of this kind of dyes in effluents is a concern of legislations in several countries. Approximately 35% of women and 10% of men in Europe, Japan and the USA have used hair colorants and great part of these compounds and derivatives are released in the environment. The volume of effluents and the unknown details about toxicity and/or genotoxity of these compounds and their derivatives have attracted much attention. The contents of hair dyes in hair coloring formulations are restricted according to Annex III of the EU Cosmetic Directive. In addition, the use of certain substances has been banned in these formulations according to Annex II of the Directive because of their toxicity and/or carcinogenicity. Therefore, efficient treatment methods of effluents containing these residues are scarce.

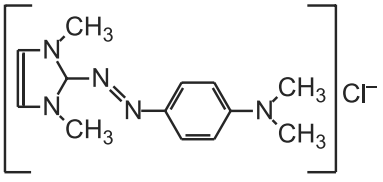

Figure 1. Molecular structure of hair dye basic red 51.

The aim of the present study is to investigate the capability of W/WO_3 semiconductor systems to degrade a basic red 51 dye, used as a model pollutant of hair dye bearing azo groups as chromophore in photoeletrocatalytic system irradiated by both ultraviolet (280-400 nm) and visible (420-630 nm) light.

Experimental

Chemicals and materials

All reagents used in preparing the solutions were of analytical grade, using distilled water purified through the Milli-Q system (18.2 MΩ cm^{-1} Millipore) in their preparation. The hair dye basic red 51 was purchased from the company Arianor. Tungsten foil (Alfa Aeser, 0.25 mm thick, 99.95%) was used as the substrate for oxide film growth.

Preparation of W/WO_3 thin film electrode

W/WO_3 electrode was prepared by anodization of tungsten foil (Alfa Aesar, 0.25 mm, 99.95%). This foil was laser cut to 2×2 cm in size and mechanically polished on SiC sandpaper of successively finer roughness (800, 1000, 1200, 1500 and 2000). After this treatment the foil was washed in ultrasonic bath for 5 min in acetone followed by isopropanol, water, dried with N_2 and immediately used.[46] For the experiments we used an anodizing conventional electrochemical cell of two-electrode, the tungsten foil (2×2 cm) as working electrode and a Pt gauze as counter-electrode. A tungsten foil was immersed in NaF solution 0.15 mol L^{-1} as the supporting electrolyte, applying a ramp potential of 0.2 V s^{-1} until it reached 60 V, which was maintained for 2 h,[28] using a power supply 60 V/2 A stabilized Tectrol®. After anodizing, the electrode was carefully washed by immersion in deionized water and dried under N_2 flow. As final treatment, the electrode was annealed at 450 °C for 30 min according to procedure described in the literature.[46]

Characterization of W/WO_3 thin film electrode

The morphological analysis of W/WO_3 surface was performed by scanning electron microscope FE-SEM high resolution with the source of electrons by field emission, JEOL, model JSM-7500-F; energy dispersive X-ray spectroscopy (EDX) and atomic force microscopy (AFM) (Digital Instruments-Veeco model MultiMode Nanoscope III_a). The scans in AFM were performed in contact mode (N3Si4 probe of Veeco model NP) and tapping mode (silicon probe of Nanoworld model NCH). The surface was also characterized by X-ray powder diffraction (XRD) with a Siemens D5000 diffractometer (CuKα radiation, λ = 1.541 Å), using a curved graphite monochromator, and a fix divergence slit of 1/8° in a Bragg-Brentano configuration. The electrode was electrochemically characterized by linear scan voltammetry using a reactor and sodium sulfate 0.10 mol L^{-1} as supporting electrolyte. The reactor was submitted to irradiation of 150 W Xe lamps (Oriel) operating under wavelength region 280-400 nm and 420-630 nm, corresponding to the ultraviolet and visible regions, respectively. The electrochemical reactor is composed of three electrodes system, containing a Pt gauze as counter-electrode, Ag/AgCl, KCl saturated as reference electrode and W/WO_3 as working electrode.

Photoelectrocatalytic study

The photoelectrocatalytic oxidation experiments were conducted in a single Teflon reactor with capacity of

30 mL. In one reactor side was inserted a quartz window of 4.0×2.5 cm positioned to receive direct light irradiation at controlled wavelength (filter 66216: 280-400 nm and 66219: 420-530 nm Oriel). In the working electrode, W/WO_3 acted as photo anode and the system was completed by a Pt gauze as counter-electrode. The system was stirred by flow of compressed air. The photoelectrocatalytic oxidation experiments were conducted for: 1.0×10^{-5} mol L^{-1} basic red 51 in 0.10 mol L^{-1} sodium sulfate pH 2.0, controlled current density of J = 1.25 mA cm^{-2}, light irradiation of 150 W xenon lamp-free ozone Oriel model 6255, operating in the ultraviolet and visible regions, respectively. The color removal was analyzed in the form of rate lows of the dye chromophore group, registering through a spectrophotometer UV-Vis linear diode array Hewlett Packard, model 8453, interfaced to an UV-visible ChemStation program Software, Hewlett Packard model HP-854X. All measurements were performed using quartz cells of 1 cm optical path at a wavelength range of 200-800 nm. The degradation of organic matter during photoelectrocatalytic oxidation was monitored by determination of total organic carbon (TOC) analyzer on a total carbon and inorganic model TOC VCP-N Shimatzu coupled to an automatic injector ASI. A galvanostat AUTOLAB PGSTAT 302 Model controlled by the software GPES was used to apply controlled current density at the photoanode during photoelectrocatalytic oxidation experiments. All pH measurements were carried out on a Corning 555 pH meter.

Results and Discussion

Morphology of W/WO_3 thin film electrode

Figure 2B shows FE-SEM images of W/WO_3 films grown by electrochemical anodizing process (2 h at 60 V) and that obtained for tungsten (substrate) (Curve A). The image observation (Figure 2B) revealed the roughness of the surface due to particles of WO_3 film on the surface of W. The nanoporous sizes are around 100 nm, which are best seen in the image capture with increased resolution, as shown in Figure 2C.

In order to diagnose possible contamination in the synthesis process of the film W/WO_3, the prepared electrode was analyzed by energy dispersive X-ray spectroscopy (EDX), revealing the relative intensity of characteristic peaks of oxygen and tungsten identified on the surface. The samples are predominantly tungsten and oxygen, without traces of fluorine, confirming the formation of W/WO_3 film without contaminants that could interfere in the efficiency of the material applied as photoanode in photoelectrocatalytic process.

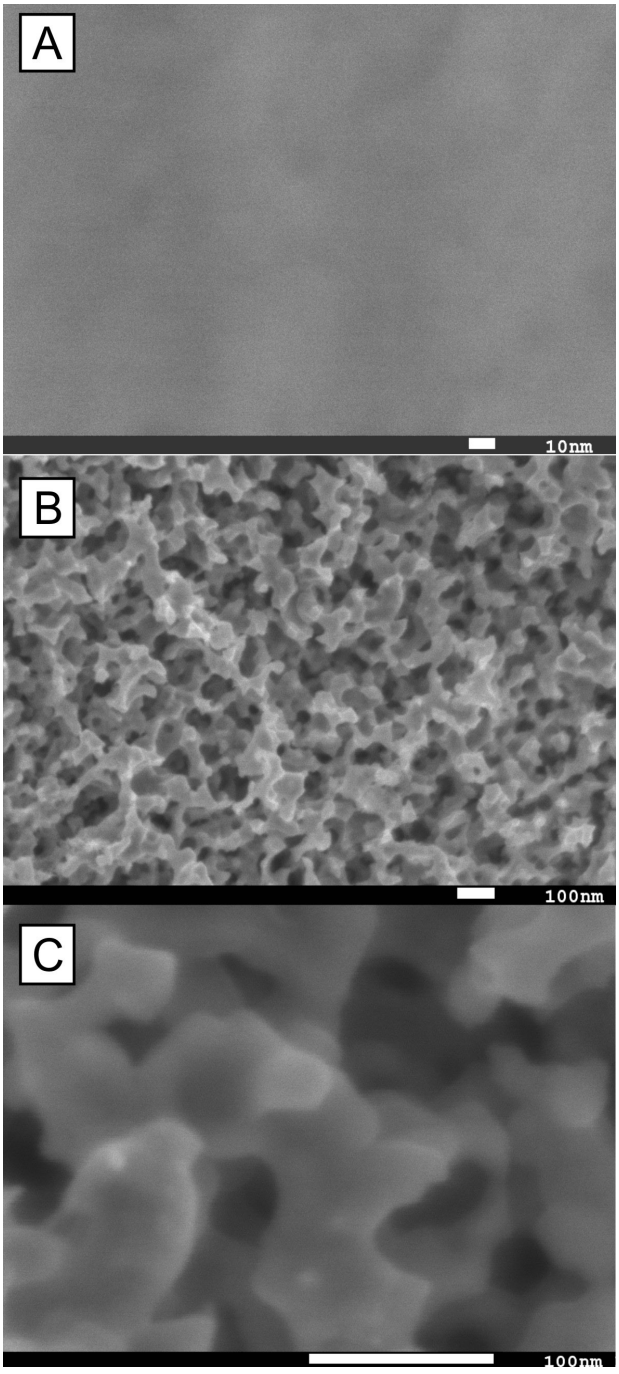

Figure 2. FE-SEM images of (A) W foil; (B) nanoporous W/WO_3 thin film electrode obtained by electrochemical anodization of tungsten foil in 0.15 mol L^{-1} NaF at 60 V for 2 h, annealed at 450 °C (30 min) and (C) magnified image of (B).

Figure 3 shows the topography in two-dimensional and three-dimensional images of W/WO_3 electrode surface by AFM, in order to elucidate possible deformations on the electrode surface. It is possible to see the great uniformity of WO_3 in nanoporous form on the substrate surface (tungsten), which is around 100 nm, also observed by FE-SEM analysis.

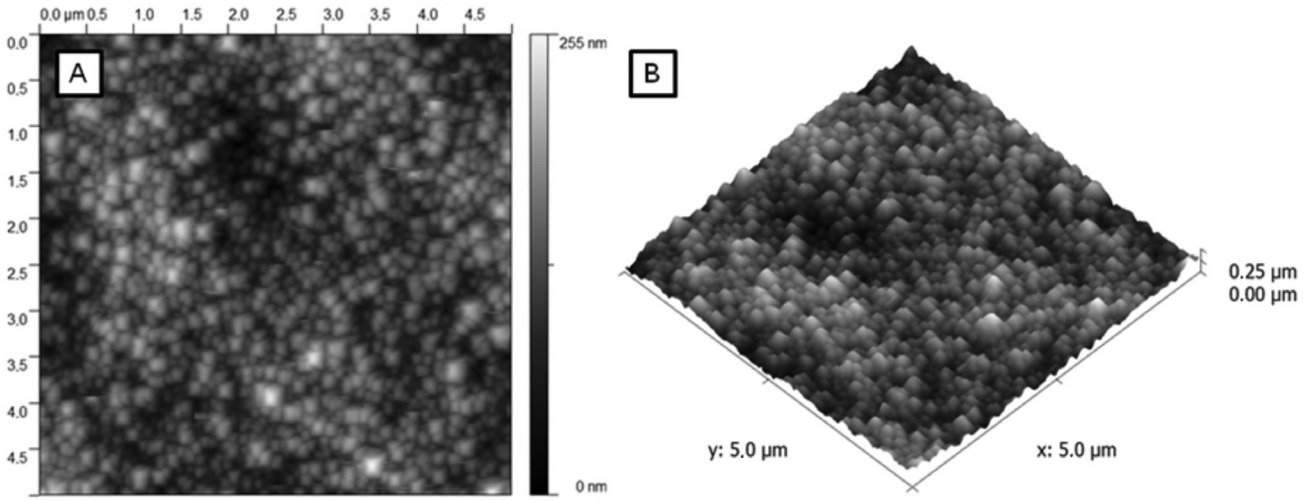

Figure 3. Atomic force microscopy images of W/WO_3 thin film electrode obtained by anodization of tungsten foil in 0.15 mol L^{-1} NaF at 60 V for 2 h, annealed at 450 °C (30 min). (A) - W foil, (B) - WO_3 in nanoporous form.

Figure 4 shows the X-ray diffraction patterns of tungsten foil (Figure 4A) and W/WO_3 samples obtained after 2 h at 60 V in 0.15 mol L^{-1} NaF, submitted to annealing at 450 °C (30 min), Figure 4B. No diffraction peaks of WO_3 appeared on the substrate (Figure 4A), but the intensities of five peaks of WO_3 on the sample prepared by anodizing process is seen on: 2θ = 23.10, 2θ = 23.66, 2θ = 24.40, 2θ = 33.26 and 2θ = 34.10. This behavior is indicative of highly-crystalline monoclinic structure of WO_3 on the substrate surface. The monoclinic phase has been reported to oxidize water and organic species under visible light.[25,47,48]

Photoactivity of W/WO_3 thin film electrode

The photoactivity of the electrode was tested recording linear voltammetric curves (0.001 V s^{-1}) immerging W/WO_3 photoanode in sodium sulfate 0.10 mol L^{-1}, under dark and irradiation of xenon lamp 150 W, operating in the ultraviolet (280-400 nm) and visible (420-630 nm) regions. The photocurrent *vs.* applied potential curves obtained are shown in Figure 5. The photocurrent intensity is neglected at dark conditions (Curve A) and shows a marked increase of photocurrent at potential higher than 0.2 V under irradiation in the ultraviolet and visible regions, with maximum values of photocurrent (E = +1.5 V) around 14 mA cm^{-2} and 18 mA cm^{-2} for ultraviolet and visible irradiation, respectively. At both conditions, there is photocurrent, indicating that photogenerated electrons (e^-) and holes (h^+)[18] are formed by irradiation. Under positive bias potential the current density drives the lacunas towards the surface of photoanode and the electrons to the counter electrode (gauze Pt), which is not photoactive.[49] This process reduces the recombination electron/hole, increases the lifetime of $OH^{\bullet}$ radicals generated on the surface of the photo anode due to water oxidation and produces high photocurrent. In both cases, the curves of I_{ph} *vs.* E increased when irradiated for either UV or visible

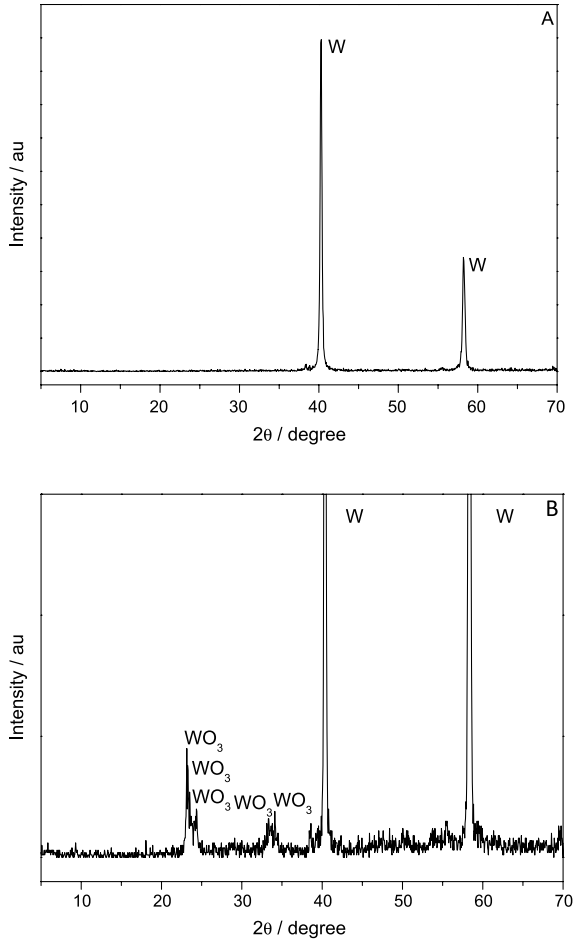

Figure 4. X-ray diffraction images obtained for W foil (A) and W/WO_3 thin film electrode (B) obtained by anodization of tungsten foil in 0.15 mol L^{-1} NaF at 60 V for 2 h.

light. This means that film of W/WO_3 structure can be activated by light of longer wavelength (2.4 to 2.8 eV),[51] without decreasing water oxidation in visible region. This is particularly important in view of the applications of a WO_3 photoanode to the photodegradation of organic effluents since the solar light intensity strongly increases through the 400 ± 500 nm wavelength regions. The literature reports[50] maximum photoactivity in the range 515-480 nm for films with highly-crystalline monoclinic structure of WO_3 with a band gap between 2.41-2.58 eV. The red-shifting of the absorption bands is consistent with the characteristic values given for WO_3 monoclinic structure.[50,51] This behavior suggests that the proposed method to obtaining films of WO_3 is a good strategy to increase the light absorption in the long wavelength region above 480 nm.

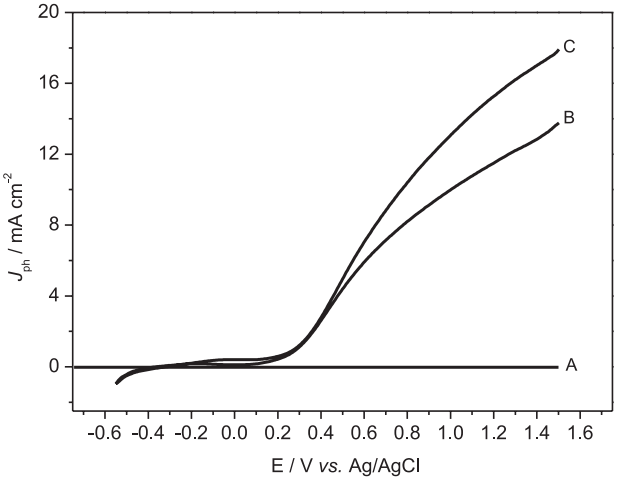

Figure 5. Photocurrent/potential curves obtained for W/WO_3 thin film electrode in Na_2SO_4 0.1 mol L^{-1}, without (A) and under visible (C) and ultraviolet irradiation (B). $\nu = 0.001$ V s^{-1}.

The incident photon to electron conversion efficiency (IPCE) was evaluated for WO_3 irradiated on visible and UV source. The IPCE (incident photon to current efficiency) calculated by; ICPE = (1240J / Pλ) × 100, where J = photocurrent density (mA cm^{-2}), P = light power (mW cm^{-2}) and λ = wavelength (nm), using current values taken on potential of 1.5 V, *vs.* Ag/AgCl at pH 2.0 in 0.1 mol L^{-1} Na_2SO_4) and values of irradiation monitored at λ of 380 nm (ultraviolet) and 490 nm (visible). The corresponding values of IPCE obtained were 106 ± 8.5% and 45 ± 2.1%, respectively. Note that values of IPCE higher than 100% are obtained and such values are consistent with the ''current-doubling'' nature.[52,53] These comparative data can be diagnostic of the much better performance of WO_3 at higher wavelengths, but there is current doubling effect. Irradiation of wavelengths smaller than 490 nm penetrates less into the film, these trends also translate to a lower surface recombination for the photocarriers in WO_3. Therefore, better separation of electrons/roles in the photoactivity is expected.

Photoelectrocatalytic oxidation of basic red 51

The photoelectrocatalytic oxidation of 1.0×10^{-5} mol L^{-1} basic red 51 dye solution was conducted in 0.10 mol L^{-1} Na_2SO_4 pH 2.0 under controlled current density of 1.25 mA cm^{-2} with W/WO_3 photoanode irradiated by ultraviolet (280-400 nm) and visible (420-630 nm) light. Figure 6 shows the UV-Vis spectra obtained before and after 120 min of photoelectrocatalytic oxidation for the system irradiated by ultraviolet or visible light. The original spectra obtained for basic red 51 hair dye exhibited two main bands: one assigned to the centers of the unsaturated aromatic molecule in the UV region (294 nm) and the other in the visible region (524 nm) due to the azo chromophore group (-N=N-).

The results indicate that the coloration of the dye solution is completely removed when treated by photoelectrocatalytic

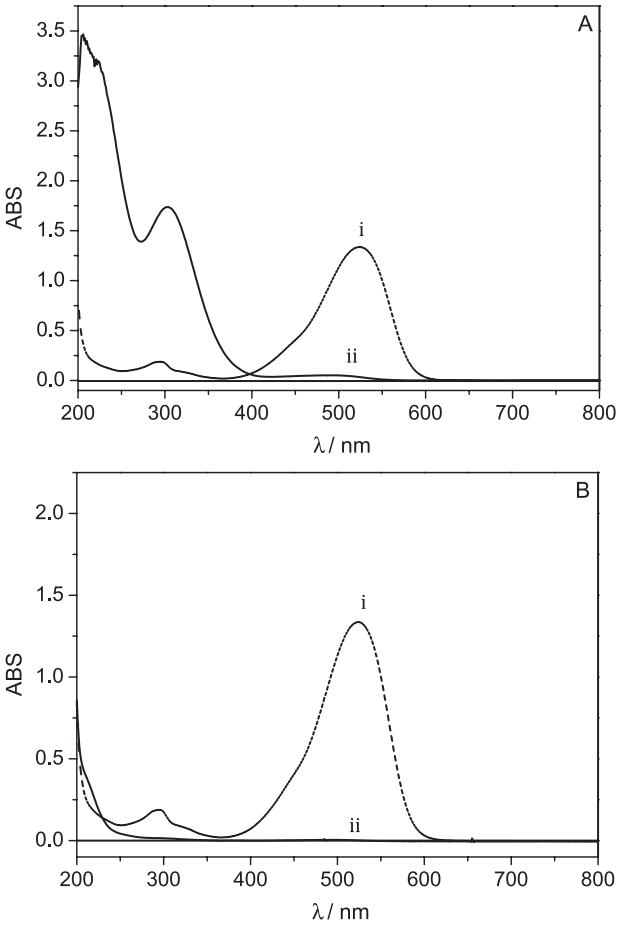

Figure 6. UV-visible spectra obtained for 1.0×10^{-5} mol L^{-1} basic red 51 dye before (*i*) and after 120 min (*ii*) of photoelectrocatalytic oxidation in: sodium sulfate pH 2.0, current density 1.25 mA cm^{-2}, under ultraviolet irradiation (A) and visible irradiation (B) regions.

oxidation using both systems of irradiation. The removal of all bands in the UV region was also observed. The photoelectrocatalytic decomposition of the basic red 51 dye in 0.1 mol L^{-1} Na_2SO_4 pH 2 was followed by measuring the degradation in 524 nm (Figure 7A). Although both systems present total color removal after 120 min, 100% discoloration was observed after 60 min of treatment of 1.0×10^{-5} mol L^{-1} basic red for W/WO_3 photoanode irradiated by visible light, Figure 7B, while only 70% was obtained under irradiation of ultraviolet region, Figure 7A. These results explain the higher photoactivity for W/WO_3 photoexcited with visible irradiation.

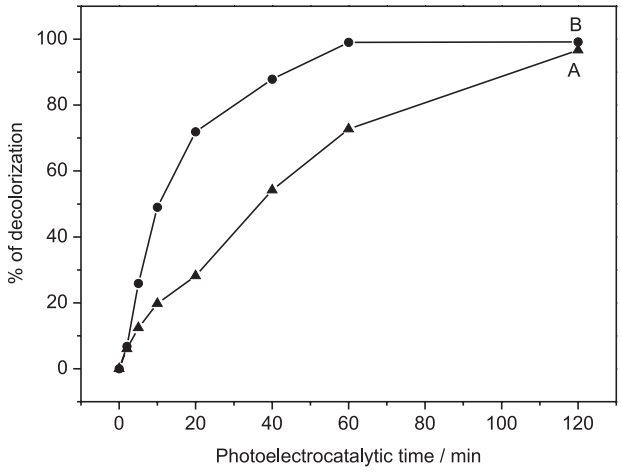

Figure 7. Discoloration percentage, λ_{max} = 524 nm, of 1.0×10^{-5} mol L^{-1} dye basic red 51, 0.10 mol L^{-1} in Na_2SO_4, pH 2.0. Photoelectrocatalytical oxidation conditions: Current density of 1.25 mA cm^{-2}, Irradiation (280-400 nm) (A) and visible (420-630 nm) light (B).

Graphs of absorbance reduction as a function of time was plotted as ln $[A]_t/[A]$ *vs.* t following discoloration at 524 nm. All curves obtained showed linear relationship up to 120 min of photoelectrocatalysis for dye degradation under irradiation at UV region and visible region, which is a typical behavior of a pseudo first order reaction in dye consumption. The constant discoloration rates obtained were –0.031 min^{-1} and –0.064 min^{-1}. The higher discoloration rate observed for W/WO_3 when irradiated at wavelenght of 420-630 nm was interesting and can be explained by other phenomenon occurring on electrode surface.[54] Conventional nano-dimensional semiconductor photocatalysts degrade organic pollutants through a series of charge transfers, according to: *i*) reaction between the photogenerated hole and water to produce the potent oxidant agent, hydroxyl radical $OH^{\bullet}$ as shown in equations 1 and 2:[55,56]

$$WO_3 + h\nu \rightarrow WO_3{-}e^-_{BC} + WO_3{-}h^+_{BV} \quad (1)$$

$$WO_3{-}h^+_{BV} + H_2O_{ads} \rightarrow WO_3{-}OH^{\bullet}_{ads} + H^+ \quad (2)$$

ii) reaction between the lacunas and adsorbed pollutant on catalyst surface:

$$P_{ads} + WO_3{-}h^+_{BV} \rightarrow P^{\bullet} + H^+ \quad (3)$$

However, the mechanism occurring in equation 2 is more accepted in the literature due to the reduced longevity generated role in photoanode surface, in the photoseconds order with the photoelectrocatalytic oxidation of the basic red 51 over hydroxyl radicals.

Nevertheless, the higher efficiency observed for dye degradation when W/WO_3 electrode is photoexcited with visible radication can be explained due to other phenomenon taking place in the mechanism. The chemistry of tungsten oxide reveals a second potential mechanism for pollutant degradation WO_3, when they can present in mixed oxidation states and can also act as an oxidizing agent, as shown in equation 4:

$$e^- + H^+ + WO_3 \rightarrow H_xW^{6+}_{(1-x)}\,W^{5+}_xO_3 \quad (4)$$

The reduction of W^{6+} to W^{5+} occurs due to absorption of light with energies in the range 2.4-2.8 eV,[57] as diagnosed by their electrochromic properties. The adsorption of dye on electrode surface and the oxidizing power of $H_xW^{6+}_{(1-x)}\,W^{5+}_xO_3$ are analogous to the description given for methanol oxidation and methylene blue treated by photoelectrochemistry on WO_3 electrodes.[54] This could be amplifying to the effect expected for a system operating under $OH^{\bullet}$ generation on W/WO_3 surface.

In order to test the mineralization degree obtained after 120 min of treatment by photoelectrocatalytic oxidation of hair dye (1.0×10^{-5} mol L^{-1}) in Na_2SO_4 (0.1 mol L^{-1}) at pH 2.0 the TOC removal was measured in both solution. Only 40% of the total organic carbon (TOC) removal was observed on system activated by UV irradiation and 63% on system irradiated by visible light. This behavior indicates that photoelectrocatalysis technique would be a good option not only to decolorize the solution but also to mineralize the organic material. Besides, there is a significant gain on irradiation by visible light on electrode surface during dye treatment. This effect provides an opportunity for the sustainable solar assisted remediation of organic contaminated water bodies for hair dyes.

Conclusions

Our findings indicate that W/WO_3 thin films can be grown by electrochemical anodization on W foil and it is the base to form photoanodes with uniform nanoparticles of 100 nm. The best conditions to form crystalline W/WO_3

films were obtained during anodization in 0.15 mol L^{-1} NaF electrolyte at 60 V during 2 h. The photoanode presents good photoactivity when illuminated by both region wavelenght from 280-400 nm (UV light) and visible region 420-630 nm. The photoanode was tested in removal of basic red 51, widely used as dye in temporary and semi-permanent hair dyeing. It is possible to get 100% discoloration of 1.0×10^{-5} mol L^{-1} dye solution, after 60 min when treated using irradiation under visible region, and after 120 min of treatment under irradiation in ultraviolet region. The discoloration follows a kinetics of pseudo-first order with constant rate of k = –0.064 and –0.031 min^{-1} for both systems, respectively. The TOC removal obtained for both systems were 63% and 40%, respectively, indicating that the process is more efficient when operating under visible irradiation of the W/WO_3 photoanode. The phenomenon can be explained due to electrochromic properties of the WO_3 that can act as an oxidizing agent, when irradiated by visible light. The process can be an effective alternative to treat effluents containing hair dyes residues mainly from basic dye family. Further studies are in progress to test the risk of forming by-products.

Acknowledgments

The authors thank FAPESP, CNPq and CAPES for the financial support of this work.

References

1. Hepel, M.; Luo, J.; *Electrochim. Acta* **2001**, *47*, 729.
2. Yu, J.; Qi, L.; Cheng, B.; Zhao, X.; *J. Hazard. Mater.* **2008**, *160*, 621.
3. Rajeshwar, K.; Tacconi, N. R. In *Interfacial Electrochemistry. Theory, Experiment and Applications*; Wieckowski, A. ed., Marcel Dekker: New York, 1999, pp. 721-736.
4. Zanoni, M. V. B.; Sene, J. J.; Anderson, M. A.; *J. Photochem. Photobiol., A* **2003**, *157*, 55.
5. Carneiro, P. A.; Osugi, M. E.; Sene, J. J.; Anderson, M. A.; Zanoni, M. V. B.; *Electrochim. Acta* **2004**, *49*, 3807.
6. Osugi, M. E.; Umbuzeiro, G. A.; Anderson, M. A.; Zanoni, M. V. B.; *Electrochim. Acta* **2005**, *50*, 5261.
7. Osugi, M. E.; Umbuzeiro, G. A.; Castro, F. J. V.; Zanoni, M. V. B.; *J. Hazard. Mater*. **2006**, *137*, 871.
8. Osugi, M. E.; Rajeshwar, K.; Ferraz, E. R. A.; Oliveira, D. P.; Araújo, A. R.; Zanoni, M. V. B.; *Electrochim. Acta* **2009**, *54*, 2086.
9. Oliveira, A. P.; Carneiro, P. A.; Sakagami, M. K.; Zanoni; M. V. B.; Umbuzeiro, G. A.; *Mutat. Res.* **2007**, *626*, 135.
10. Fraga, L. E.; Anderson, M. A.; Beatriz, M. L. P. M. A.; Paschoal, F. M. M.; Romão, L. P.; Zanoni, M. V. B.; *Electrochim. Acta* **2009**, *54*, 2069.
11. Cruz, A. M.; Martínez, D. S.; Cuéllar, E. L.; *Solid State Sci.* **2010**, *12*, 88.
12. Yu, J.; Qi, L.; *J. Hazard. Mater*. **2009**, *169*, 221.
13. Hong, X. T.; Wang, Z. P.; Cai, W. M.; Lu, F.; Zhang, J.; Yang, Y. Z.; Ma, N.; Liu, Y. J.; *Chem. Mater*. **2005**, *17*, 1548.
14. Yu, J. C.; Yu, J. G.; Ho, W. K.; Jiang, Z. T.; Zhang, L. Z.; *Chem. Mater*. **2002**, *14*, 3808.
15. Sayama, K.; Hayashi, H.; Arai, T.; Yanagida, M.; Gunji, T.; Sugihara, H.; *Appl. Catal., B* **2010**, *94*, 150.
16. Hong, S. J.; Jun, H., Borse, P. H.; Lee, J. S.; *Int. J. Hydrogen Energy* **2009**, *34*, 3234.
17. Marsen, B.; Miller, E. L.; Paluselli, D.; Rocheleau, R. E.; *Int. J. Hydrogen Energy* **2007**, *32*, 3110.
18. Somasundaram, S.; Chenthamarakshan, R.; Tacconi, N. R.; Basit, N. A., Rajeshwar, K.; *Electrochem. Commun*. **2006**, *8*, 539.
19. Colton, R. J.; Guzman, A. M.; Rabalais, J. W.; *J. Appl. Phys.* **1978**, *49*, 409.
20. Yous, B.; Robin, S.; Donnadieu, A.; Dufour, G.; Maillot, C.; Roulet, H.; Senemaud, C.; *Mater. Res. Bull*. **1984**, *19*, 1349.
21. Sivakumar, R.; Moses, Ezhil Raj, A.; Subramanian, B.; Jayachandran, M.; Trivedi, D. C.; Sanjeeviraja, C.; *Mater. Res. Bull*. **2004**, *39*, 1479.
22. Santato, C.; Odziemkowski, M.; Ulmann, M.; Augustynski, J.; *J. Am. Chem. Soc*. **2001**, *123*, 10639.
23. Wang, H.; Lindgren, T.; He, J.; Hagfeldt, A.; Lindquist, S. E.; *J. Phys. Chem. B* **2006**, *104*, 5686.
24. Santato, C.; Ulmann, M.; Augustynski, J.; *Adv. Mater*. **2001**, *13*, 511.
25. Santato, C.; Augustynski, M. J.; *J. Phys. Chem. B* **2001**, *105*, 936.
26. Yamanaka, K.; Oakamoto, H.; Kidou, H.; Kudo, T.; *Jpn. J. Appl. Phys. Part 1, Regul. Pap. Short Notes Rev. Pap*. **1986**, *25*, 1420.
27. Bellac, D. L.; Azens, A.; Granqvist, C. G.; *Appl. Phys. Lett*. **1995**, *66*, 1715.
28. Watcharenwong, A.; Chanmane, W.; Tacconi, N. R.; Chenthamarakshan, C. R.; Kajitvichyanukul, P.; Rajeshwar, K.; *J. Electroanal. Chem*. **2008**, *612*, 112.
29. Yang, B.; Li, H.; Blackford, M.; Luca, V.; *Curr. Appl. Phys*. **2006**, *6*, 436.
30. Baeck, H.; Choi, K.-S.; Jaramillo, T.F.; Stucky, G.D.; McFarland, E.W.; *Adv. Mater*. **2003**, *15*, 1269.
31. Shen, P. K.; Tseung, A. C. C.; *J. Mater. Chem*. **1992**, *2*, 1141.
32. Yagi, M.; Sone, K.;Yamada, M.; Umemiya, S.; *Chem. Eur. J.* **2005**, *11*, 767.
33. Yagi, M.; Umemiya, S.; *J. Phys. Chem. B* **2002**, *106*, 6355.
34. Sone, K.; Konishi, K.; Yagi, M.; *Chem. Eur. J.* **2006**, *12*, 8558.
35. Shen, P. K.; Tseung, A. C. C.; *J. Electrochem. Soc*. **1994**, *141*, 3082.
36. Shen, P. K.; Chen, K. Y.; Tseung, A. C. C.; *J. Chem. Soc., Faraday Trans*. **1994**, *90*, 3089.

37. Shen, P. K.; Chen, K. Y.; Tseung, A. C. C.; *J. Electroanal. Chem.* **1995**, *389*, 223.
38. Bock, C.; MacDougall, B.; *Electrochim. Acta* **2002**, *47*, 3361.
39. Waldner, G.; Bruger, A.; Gaikwad, N. S.; Neumann-Spallart, M.; *Chemosphere* **2007**, *67*, 779.
40. Luo, J.; Hepel, M.; *Electrochim. Acta* **2001**, *46*, 2913.
41. Hepel, M.; Hazelton, S.; *Electrochim. Acta* **2005**, *50*, 5278.
42. Lina, C-F.; Wub, C-H.; Onna, Z-N.; *J. Hazard. Mater.* **2008**, *154,* 1033.
43. Georgieva, J.; Armyanov, S.; Valova, E.; Tsacheva, Ts.; Poulios, I.; Sotiropoulos, S.; *J. Electroanal. Chem.* **2005**, *585*, 35.
44. Masukawa, Y.; *J. Chromatogr., A* **2006**, *1108*, 140.
45. Robbins, C. R.; *Chemical and Physical Behavior of Human Hair*, 4th ed. Spring Verlag: New York, 2002.
46. de Tacconi, N. R.; Chenthamarakshan, C. R.; Yogeeswaran, G.; Watcharenwong, A.; de Zoysa, R. S.; Basit, N. A.; Rajeshwar, K.; *J. Phys. Chem. B* **2006**, *110*, 25347.
47. Abe, R.; Takami, H.; Murakami, N.; Ohtani, B.; *J. Am. Chem. Soc.* **2008**, *130*, 7780.
48. Solarska, R.; Santato, C.; Jorand-Sartoretti, C.; Ulmann, M.; Augustynski, J.; *J. Appl. Electrochem*. **2005**, *35*, 715.
49. Tsuchiya, H.; Macak, J. M.; Muller, L.; Kunze, J.; Muller, F.; Greil, P.; Virtanen, S.; Schmuki, P.; *J. Biomed. Mater. Res. A* **2006**, *77*, 534.
50. Bamwenda, G. R.; Arakawa H.; *Appl. Catal. A* **2001**, *210*, 181.
51. Granqvist, C. G.; *Sol. Energy Mater. Sol. Cells* **2000**, *60*, 201.
52. Morrison, S. R.; Freund, T.; *J. Chem. Phys*. **1967**, *47*, 1543.
53. Gomes, W. P.; Freund, T.; Morrison, S. R.; *J. Electrochem. Soc.* **1968**, *115*, 818.
54. Macphee, D. E.; Rosemberg, D.; Skellern, M. G.; Wells, R. P.; Duffy, J. A.; Killham, K. S.; *J. Solid State Electrochem*. DOI 10.1007/s10008-010-1062-4. Published online on 20 April 2010.
55. Martin, S. T.; Herrmann, H.; Choi, W.; Hoffmann, M. R.; *Trans. Faraday Soc*. **1994**, *9l*, 3315.
56. Hoffman, M. R.; Martin, S. T.; Choi, W.; Bahnemann, D. W.; *Chem. Rev*. **1995**, *95*, 69.
57. Finley, H. O.; *Semiconductor Electrodes*, Elsevier: Amsterdam, 1988, p. 519.

Submitted: July 28, 2010
Published online: January 18, 2011

FAPESP has sponsored the publication of this article.